

**Fig. 4. Western blot analysis of extracts from mouse tissues.** Western blot was performed using (A), an anti-AKR1B1 antibody; (B) an anti-AKR1C3 antibody. The AKR1B1 protein was strongly expressed in the brain, heart, lung, and kidney; however, the anti-AKR1B1 antibody could not be recognized in liver lysate. The AKR1C3 protein was strongly expressed in the liver and kidney but not in the brain. Lower panels show immunostaining of  $\beta$ -actin using the same membrane. Ten micrograms of lysate protein of each tissue was used.

brain extracts from the cerebellar cortex, spinal cord, substantia nigra, hippocampus, hypothalamus and caudate nucleus and liver lysate were performed. The tissues were homogenized in a 20 mM potassium phosphate buffer (pH 7.0) containing 1 tablet/50 ml protease inhibitor cocktail (Roche) and 0.05% Igepal CA-630 (Sigma). The homogenates were then centrifuged at  $15,000 \times g$  for 20 min, and solid ammonium sulfate was added to the supernatant to 70% saturation. The precipitate was collected by centrifugation at  $15,000 \times g$  for 20 min and dissolved in 0.3 vol. of the extracted buffer. The solution was dialysed overnight against the same buffer and centrifuged at  $15,000 \times g$  for 20 min. The supernatant was stored at  $-70^\circ\text{C}$  until used. The extract was subjected to 12% SDS-PAGE, and the proteins were transferred to a PVDF membrane (Bio-Rad) at 80 mA for 120 min. After being blocked with 3% skim milk, the membranes were first incubated with an adequate dilution of the antibodies and then with anti-rabbit IgG conjugated to horseradish peroxidase. Following repeated washing of the membrane, the signals were visualized with ECL plus (GE Healthcare).

**Immunohistochemistry**—Three-week-old male mice of BALB/c were purchased from a breeder (Japan SLC, Inc., Hamamatsu, Japan). They were deeply anesthetized with diethyl ether and subsequently sacrificed by perfusion with physiological saline followed by 4% paraformaldehyde in a 0.1 M phosphate buffer (pH 7.4). The brain and liver were dissected 30 min after perfusion, post-fixed in the same fixative overnight at  $4^\circ\text{C}$ , and rinsed three times at 30 min intervals with a 0.1 M phosphate buffer. They were then automatically processed through paraffin embedding with a vacuum infiltration processor (Tissue-Tek VIP5 Jr., Sakura FineTek Japan). Four serial sections of a median plane

in the liver were cut to a thickness of  $5 \mu\text{m}$  with a sliding microtome (Microm HM 430, Zeiss, Germany). The first slide was stained with the hematoxylin-eosin (HE) stain. Brain sections in the sagittal, cross (transversal) and horizontal planes were cut into serial sections with a thickness of  $5 \mu\text{m}$  with a sliding microtome. The first slide was stained with the Kluver-Barrera's (KB) stain. The second to fourth slides were used for immunostaining. After treatment with 0.3%  $\text{H}_2\text{O}_2$  in methanol, the sections were incubated overnight with anti-AKR1B1 antisera (1:200 dilution) for the second slide, anti-AKR1C3 antisera (1:200 dilution) for the third slide, and normal rabbit serum (1:200 dilution) for the fourth slide at  $4^\circ\text{C}$ . They were incubated with goat anti-rabbit peroxidase-conjugated immunoglobulin (IgG) [N-Histofine Simple Stain Mouse MaxPO(R), Nichirei Biosciences, Inc., Japan]. The peroxidase activity was visualized with 3,3'-diaminobenzidine tetrahydrochloride (DAB) in 0.05 M Tris (pH 7.6) with  $\text{H}_2\text{O}_2$  as a chromogen solution, and the sections were counterstained with the hematoxylin stain.

**Assay of Sepiapterin Reductase Activity**—The reaction mixture contained the following components: a 50 mM potassium phosphate buffer (pH 7.0), 1 mM NADPH,  $15 \mu\text{M}$  sepiapterin, 0.5 mM N-acetyl serotonin (NAS, a potent inhibitor of SPR) or DW, and an appropriate amount of human liver extract from P04 or mouse liver extract in a final volume of  $100 \mu\text{l}$ . The reaction mixture was incubated at  $37^\circ\text{C}$  for 20 min in darkness. The reaction was stopped by the addition of  $10 \mu\text{l}$  of a 20% trichloroacetic acid solution and  $20 \mu\text{l}$  of an iodine solution (1%  $\text{I}_2$ , 2% KI). After allowing the mixture to stand for 30 min at room temperature in darkness, excess iodine was reduced by the addition of  $10 \mu\text{l}$  of a 2% ascorbic acid solution (23), and the mixture was centrifuged at  $15,000 \times g$  for 5 min. The amount of biopterin (BP) in the resulting supernatant was measured by HPLC with fluorometric detection, as previously described (12).

**Assay of Tetrahydropterin-Producing Activity**—Analysis of tetrahydropterins was performed by HPLC with electrochemical detection, as described previously (14, 15). The reaction mixture contained the following components: a 50 mM potassium phosphate buffer (pH 7.0),  $100 \mu\text{M}$  NADPH,  $10 \mu\text{l}$  of a concentrated solution of PPH<sub>4</sub> synthase, 5 mM dithiothreitol, 8 mM  $\text{MgCl}_2$ ,  $14 \mu\text{M}$   $\text{NH}_2\text{TP}$ , 0.5 mM NAS and an appropriate amount of human liver extract from P04 or mouse liver extract in a final volume of  $100 \mu\text{l}$ . The reaction mixture was flushed with  $\text{N}_2$  gas, sealed, and incubated at  $37^\circ\text{C}$  for 30 min in darkness. The reaction was stopped by the addition of  $10 \mu\text{l}$  of a 20% trichloroacetic acid solution and the mixture was centrifuged at  $15,000 \times g$  for 5 min. The amount of tetrahydropterins in the resulting supernatant was measured by HPLC, as previously described (12).

## RESULTS

**Specificity of Anti-AKR1B1 and Anti-AKR1C3 Antibodies**—To demonstrate the ability of the antibodies to specifically distinguish AKR1B1 and AKR1C3 from other cellular proteins, western blot analysis was

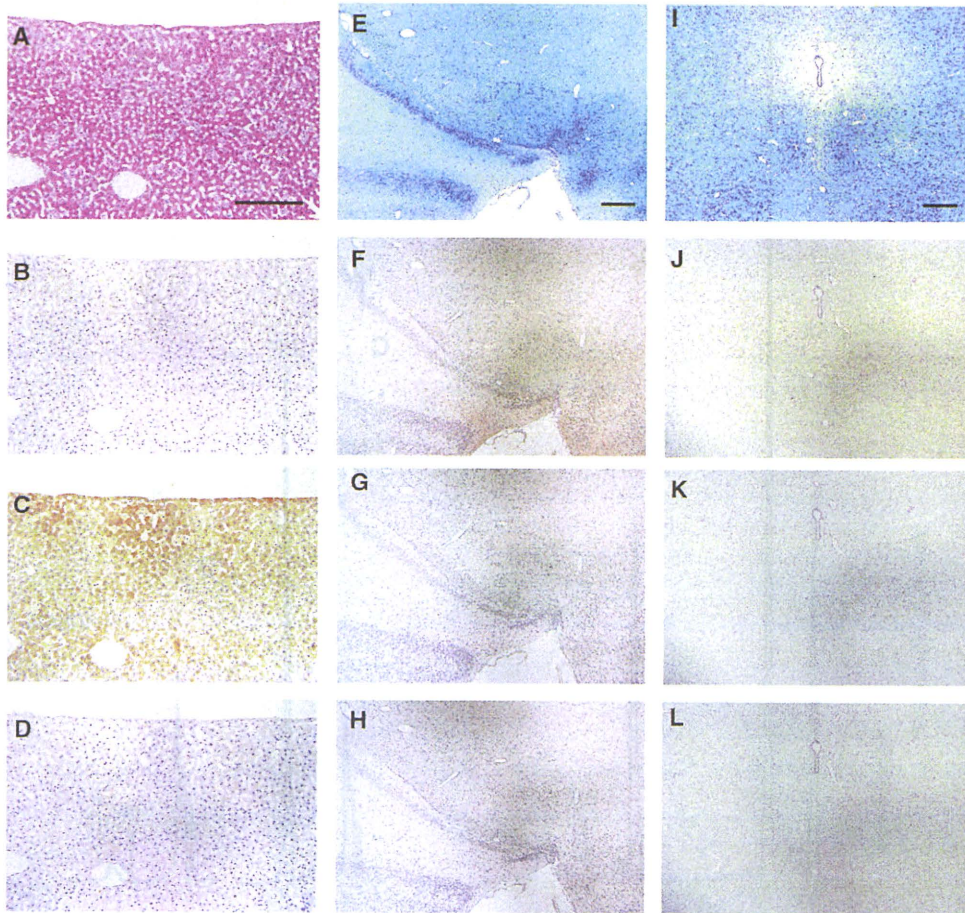
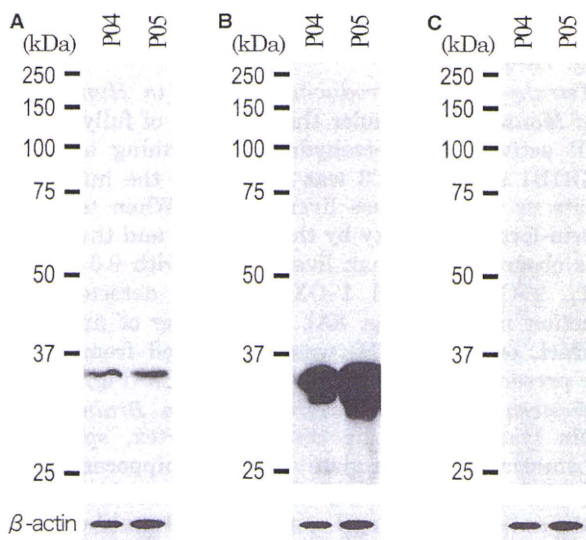


**Fig. 5. Immunohistochemical analysis of AKR1B1 and AKR1C3 in mouse liver and brain.** Paraformaldehyde-fixed paraffin sections of liver were reacted with: (A) hematoxylin-eosin (HE) stain; (B) anti-AKR1B1 serum; (C) anti-AKR1C3 serum; (D) negative control. The substantia nigra (dopaminergic neuron) sections were reacted with (E); KB stain; (F) anti-AKR1B1 serum; (G) anti-AKR1C3 serum; (H) negative control. The dorsal nucleus raphe (serotonergic neuron) sections were reacted with (I); KB stain; (J) anti-AKR1B1 serum; (K) anti-AKR1C3

serum; (L) negative control. The cross-reacting protein was visualized with 3,3'-diaminobenzidine tetrahydrochloride. The immunoreactivity of AKR1C3 is shown in the cell bodies of mouse liver. AKR1B1 immunoreactivity is not shown elsewhere in the liver regions. On the contrary, AKR1B1 immunoreactivity is shown weakly in the cell bodies of monoaminergic neurons in the brain. No staining is shown in the sections of mouse brain incubated with an anti-AKR1C3 antibody.



performed in the total cellular lysate from *E. coli* cells that expressed human AKR1B1 or AKR1C3. A single protein species with a molecular mass of ~36 kDa was detected in this total cellular preparation (Fig. 3, lanes 2 and 4). The recognized protein species had the same size as the AKR1B1 and AKR1C3 proteins (24, 25).

**Western Blot Analysis from Mouse Tissues**—Western blot analysis showed strong expression of the AKR1B1 protein in the brain, heart, lung and kidney. However, the anti-AKR1B1 antibody could not be recognized against the liver lysate (Fig. 4A). On the other hand,

**Fig. 6. Western blot analysis of human liver lysate.** Western blot was performed using (A), an anti-AKR1B1 antibody; (B) an anti-AKR1C3 antibody; and (C), a normal rabbit serum. Lower panels show immunostaining of  $\beta$ -actin using the same membrane. Both AKR1B1 and AKR1C3 proteins were detected with each antibody from the human liver lysate. Ten micrograms of lysate protein was used.

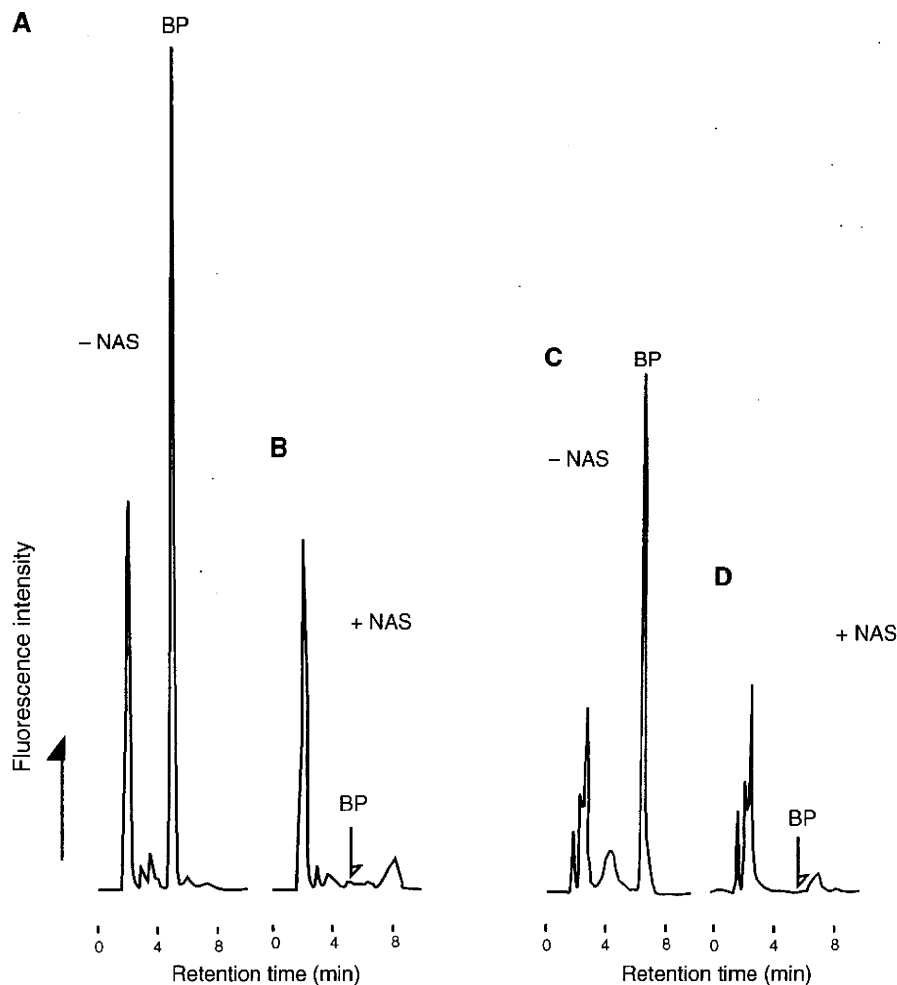


Fig. 7. Analysis by HPLC of SPR activity. The reaction mixture contained 15  $\mu$ M sepiapterin, 1mM NADPH, 0.5 mM NAS or DW, and an appropriate amount of human liver extract from P04 or an appropriate amount of mouse liver extract in a final

volume of 100  $\mu$ l. It was incubated for 20 min at 37°C in darkness. The SPR activity was measured in terms of the amount of biopterin (BP) produced by fluorimetry. (A, B) human liver extract; (C, D) mouse liver extract.

the AKR1C3 protein was strongly expressed in the liver and kidney but not in the brain (Fig. 4B).

**Immunohistochemical Analysis of AKR1B1 and AKR1C3 in Mouse Liver and Brain**—AKR1B1 immunoreactivity was not shown in the liver, but AKR1C3 immunoreactivity was shown in the cell bodies of the liver (Fig. 5A–D). In some monoaminergic neurons in the brain, AKR1B1 immunoreactivity weakly showed cell bodies of the substantia nigra and dorsal nucleus raphe, but AKR1C3 immunoreactivity could not be detected in some monoaminergic neurons in the brain, as in the negative control (Fig. 5E–L).

**Western Blot Analysis from Human Liver**—Western blot analysis for AKR1B1 and AKR1C3 was conducted in human brain and liver lysates. Both AKR1B1 and AKR1C3 proteins were detected with each antibody from the human liver lysate but not in the negative control (Fig. 6A–C).

**Sepiapterin Reductase Activity in Human Liver and Mouse Liver**—The BP-forming activity by SPR was assayed in human liver or mouse liver extracts. Strong

SPR activity was shown in human liver and mouse liver; however, the activity was completely inhibited by the addition of 0.5 mM NAS in the reaction mixture (Fig. 7A–D).

**Tetrahydropterin-Producing Activity in Human Liver and Mouse Liver**—Under the condition of fully inhibited SPR activity, the tetrahydropterin-forming activity by AKR1B1 and AKR1C3 was assayed in the human liver lysate or in the mouse liver extract. When tetrahydropterin-forming activity by the AKR1B1 and the AKR1C3 was observed in human liver extract with 0.5 mM NAS, BH<sub>4</sub>, 2'-OXPH<sub>4</sub>, and 1'-OXPH<sub>4</sub> were detected in the reaction mixture (Fig. 8A). In the case of mouse liver extract, only 2'-OXPH<sub>4</sub> was synthesized from PPH<sub>4</sub> in the presence of 0.5 mM NAS by AKR1C3 (Fig. 8B).

**Western Blot Analysis from Human Brain**—Human brain lysates from the cerebellar cortex, spinal cord, substantia nigra, caudate nucleus, hippocampus and hypothalamus were subjected to western blot analysis with anti-AKR1B1 and anti-AKR1C3 antibodies and normal rabbit serum. The anti-AKR1B1 antibody could

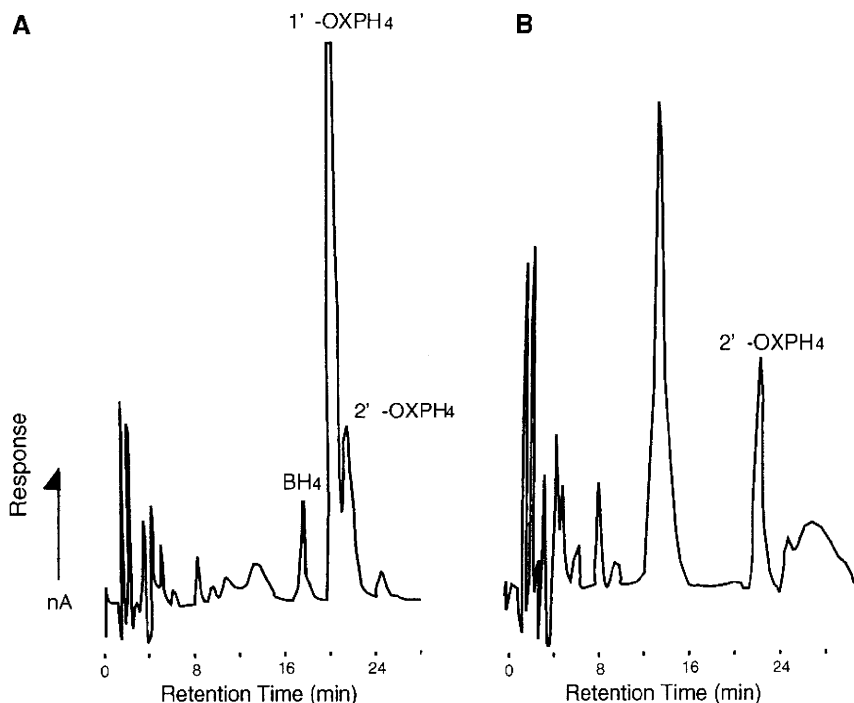


**Fig. 8. Production of BH<sub>4</sub>, 2'-OXPH<sub>4</sub>, and 1'-OXPH<sub>4</sub> by human liver or mouse liver extracts.** The reaction mixture contained the following components: a 50 mM potassium phosphate buffer (pH 7.0), 100 μM NADPH, 10 μl of a concentrated solution of PPH<sub>4</sub> synthase, 5 mM dithiothreitol, 8 mM MgCl<sub>2</sub>, 14 μM NH<sub>2</sub>TP, 0.5 mM NAS and an appropriate amount of

human liver extract from P04 or an appropriate amount of mouse liver extract in a final volume of 100 μl. The reaction mixture was flushed with N<sub>2</sub> gas, sealed and incubated at 37 °C for 30 min in darkness. The products were analysed by HPLC with electrochemical detection. (A) human liver extract; (B) mouse liver extract.

detect a major band of ~36 kDa in the extract from the cerebellar cortex, spinal cord, substantia nigra, caudate nucleus, hippocampus and hypothalamus (Fig. 9A). The AKR1B1 protein was widely detected in the human brain; however, the AKR1C3 protein was scarcely detected in the brain, in contrast to the case of the negative control (Fig. 9B and C).

#### DISCUSSION

In 2001, SPR deficiency was first discovered from a patient with progressive psychomotor retardation and dystonia. However, the patient showed normal urinary pterins without HPA (8). To explain this observation, Blau *et al.* (9) proposed that BH<sub>4</sub> was synthesized through salvage pathway I in the case of SPR deficiency (Fig. 1).

Recently, Yang *et al.* (16) indicated that SPR knockout mice exhibited HPA, dwarfism and impaired bodily movement. Furthermore, *Spr*<sup>-/-</sup> null mice, as reported by Takazawa *et al.* (17), also showed HPA. In spite of the fact that adequate activity of CBR and DHFR exists in mouse liver, SPR knockout mouse showed HPA. These results suggested that salvage pathway I may not be at work in mouse liver.

We have reported on a novel SPR-unrelated biosynthetic pathway (salvage pathway II) from PPH<sub>4</sub> to BH<sub>4</sub>, in which AKR1C3 and AKR1B1 work in concert (Fig. 2) (15). We believe that salvage pathway II works in human liver but not in wild-type mouse liver, since the SPR

knockout mouse showed HPA and a patient with SPR deficiency did not. Therefore, we prepared specific antibodies against AKR1B1 and AKR1C3 proteins (Fig. 3, lanes 2 and 4).

Western blot analysis from mouse tissue lysates using specific antibodies showed that the AKR1B1 protein was strongly expressed in the brain but not in the liver. The AKR1C3 protein existed in large amounts in the liver; however, it could not be detected in the brain (Fig. 4A and B). The immunohistochemical analysis of AKR1B1 and AKR1C3 in mouse liver and brain showed similar results to those of western blot analysis. AKR1C3 immunoreactivity was shown in the liver but not in monoaminergic neurons. In the case of AKR1B1, weak immunoreactivity was shown in the substantia nigra and the dorsal nucleus raphe, but not in the liver (Fig. 5). These results suggested that salvage pathway II, which was the SPR-unrelated BH<sub>4</sub> formation pathway from PPH<sub>4</sub>, does not act in mouse liver and brain.

On the other hand, both AKR1B1 and AKR1C3 proteins were detected with each antibody from the human liver lysate (Fig. 6A–C). Although AKR1B1 can reduce the 2'-keto group of both PPH<sub>4</sub> and 2'-OXPH<sub>4</sub>, AKR1C3 specifically reduces the 1'-keto group of PPH<sub>4</sub> but not the 1'-keto group of 1'-OXPH<sub>4</sub> (Fig. 2). If the PPH<sub>4</sub> is immediately reduced to 1'-OXPH<sub>4</sub> by AKR1B1, the formation of BH<sub>4</sub> does not occur in human liver because AKR1C3 cannot reduce 1'-OXPH<sub>4</sub> to BH<sub>4</sub>. To demonstrate the BH<sub>4</sub>-forming activity by salvage pathway II, the tetrahydropterin-producing activity in

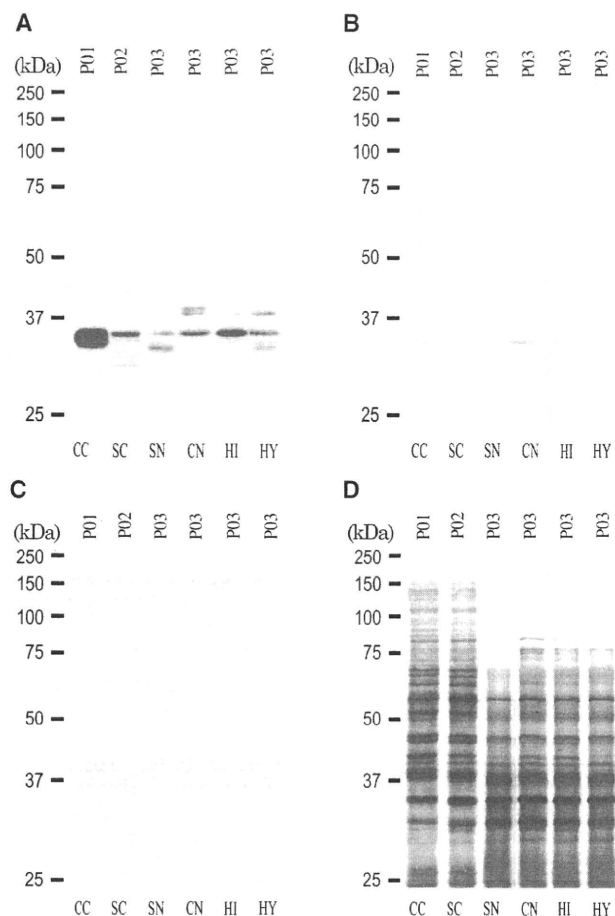


**Fig. 9. Western blot analysis of human brain lysate.** Western blot was performed using (A) an anti-AKR1B1 antibody; (B) an anti-AKR1C3 antibody; and (C) a normal rabbit serum. The gel was stained with (D) Coomassie Brilliant Blue R-250. Ten micrograms of lysate protein of the cerebellar cortex (CC), spinal cord (SC), substantia nigra (SN), caudate nucleus (CN), hippocampus (HI) and hypothalamus (HY) was used. The AKR1B1 protein was widely detected in the human brain; however, the AKR1C3 protein was scarcely detected in the brain, which contrasts the case of the negative control.

human liver and mouse liver extracts was assessed with PPH<sub>4</sub> as a substrate. First, we tried to determine the concentration on NAS, which completely inhibited SPR activity, because SPR has strong tetrahydropterin-producing activity from PPH<sub>4</sub>. In the presence of 0.5 mM NAS, SPR activity was fully suppressed in human liver and mouse liver extracts (Fig. 7A–D). When tetrahydropterin-producing activity by the AKR1B1 and the AKR1C3 was observed in human liver extract with 0.5 mM NAS, BH<sub>4</sub>, 2'-OXPH<sub>4</sub> and 1'-OXPH<sub>4</sub> were synthesized in the reaction mixture (Fig. 8A). This means that 2'-OXPH<sub>4</sub>, which is synthesized from PPH<sub>4</sub> by AKR1C3, was reduced to BH<sub>4</sub> by AKR1B1 in human liver extract. In the case of mouse liver extract, only 2'-OXPH<sub>4</sub> was synthesized from PPH<sub>4</sub> in the presence of 0.5 mM NAS by AKR1C3 (Fig. 8B). This suggests that AKR1B1, which reduces 2'-OXPH<sub>4</sub> to BH<sub>4</sub>, does not act

in mouse liver. The results of this experiment suggest that salvage pathway II, which is relevant to AKR1B1 and AKR1C3, works in human liver but not in mouse liver. In spite of adequate activity of CBR and DHFR in mouse and human liver, SPR knockout mice show HPA, and *SPR*-deficient patients do not. We have reported that the formation rate of sepiapterin from the non-enzymatic degradation of 1'-OXPH<sub>4</sub> was very slow (26) and, thus, salvage pathway I would not advance even if CBR and DHFR existed in the human and mouse liver. An *SPR*-deficient patient does not show HPA; in other words, salvage pathway II acts in the liver of the patient.

*SPR*-deficient patients displayed abnormal responses in the phenylalanine loading test, indicating that the phenylalanine hydroxylase (PAH, EC 1.14.16.1) function was somewhat impaired although the phenylalanine levels in these patients appeared to be normal (8); on the other hand, the *Spr*<sup>-/-</sup> mouse serum contained a high level of phenylalanine (16, 17). One interesting explanation for this discrepancy between the phenylalanine levels of *SPR*-deficient patients and those of *Spr*<sup>-/-</sup> mice was proposed by Yang *et al.* (16). These researchers contend that mice and humans have different levels of alternative enzyme activities that compensate for the loss of SPR; thus, a higher level of BH<sub>4</sub> (a level sufficient for the function of PAH) is produced in human liver than in mouse liver. Therefore, salvage pathway II in human liver, which is relevant to AKR1B1 and AKR1C3, is an alternative BH<sub>4</sub> formation route that compensates for the loss of SPR.

The results of western blot analysis showed that a large amount of the AKR1B1 protein was detected in human brain but the amount of the AKR1C3 protein was extremely scarce in it (Fig. 9). Penning *et al.* (27) have reported that the mRNA for AKR1C3 was expressed in many human tissues; however, the expression level of AKR1C3 mRNA in the brain was very low compared to that in other tissues.

This suggests that salvage pathway II cannot progress in human and mouse brain and that a large amount of 1'-OXPH<sub>4</sub> synthesized from PPH<sub>4</sub> by AKR1B1 accumulates in the entire brain region. These results of the expression analysis of salvage pathway II in humans and mice can explain why a patient with SPR deficiency shows progressive neurological deterioration without HPA and SPR knockout mice exhibit abnormal locomotion activity with HPA. SPR deficiency can be diagnosed by investigating the pteridine metabolites in CSF, in which the sepiapterin level is high, biopterin is mildly increased, and neopterin is normal [sepiapterin: 5–20 nmol/l, (SPR deficiency), not detectable, (normal); biopterin: 24–60 nmol/l, (SPR deficiency), 10–40 nmol/l, (normal); neopterin: 11–25 nmol/l, (SPR deficiency), 10–30 nmol/l, (normal), BIODEF database www.bh4.org]. It has been reported that the sepiapterin level was significantly elevated in the brain of *Spr*<sup>-/-</sup> mice (16). We have reported that a small amount of sepiapterin was formed in the nonenzymatic degradation of 1'-OXPH<sub>4</sub> and the rate of the nonenzymatic formation of sepiapterin from 1'-OXPH<sub>4</sub> was quite slow (15, 26). However, sepiapterin is a stable molecule in the dihydro form of pteridine

derivatives and may accumulate in the brain of *Spr*<sup>-/-</sup> mice and in the CSF of SPR-deficient patients over a long period of time. Therefore, the sepiapterin level may be elevated in the CSF of a patient with SPR deficiency and in the brain of *Spr*<sup>-/-</sup> mice. In the case of mutant mice, the amount of neopterin increased (to five times of that found in *Spr*<sup>+/+</sup> mice) in the brain (16). These results suggest that PTPS, which synthesizes PPH<sub>4</sub> from NH<sub>2</sub>TP in the brain of mutant mice, may be inhibited by the large amounts of 1'-OXPH<sub>4</sub> synthesized from PPH<sub>4</sub> by AKR1B1. In consequence, the amount of neopterin, an NH<sub>2</sub>TP metabolite, may increase in the brain of *Spr*<sup>-/-</sup> mice. Despite the large amount of 1'-OXPH<sub>4</sub> synthesized in the brain of a patient with SPR deficiency, the neopterin level was normal in the CSF of such a patient. It is not clear why the amounts of neopterin do not increase in the CSF of a patient with SPR deficiency. Furthermore, the fact that the level of biopterin, a BH<sub>4</sub> metabolite, moderately increases in the CSF of an SPR-deficient patient cannot be explained by the results of our experiment. Yang *et al.* (16) reported that the BH<sub>4</sub> level in the liver was more dramatically reduced (to 1.1% of that of the wild type) in *Spr*<sup>-/-</sup> mice than in the control, whereas a relatively mild decrease (40.5% of that of the wild type) was detected in the brain of SPR knockout mice. Similar results have been reported by Takazawa *et al.* (17). These findings suggest that an unknown quantity of SPR-unrelated BH<sub>4</sub> production may occur in the brain; therefore, the biopterin level mildly increases in the CSF of patients with SPR deficiency. Further studies on the SPR-unrelated BH<sub>4</sub> formation route will be necessary to understand the differences in the levels of pteridine metabolites in the CSF of patients with SPR deficiency and in the brain of SPR knockout mouse.

#### ACKNOWLEDGEMENTS

We are grateful to Dr Toshiharu Nagatsu (Fujita Health University School of Medicine) for his kind support.

#### FUNDING

Grant-in-Aid from the Ministry of Education, Culture, Sports, Science, and Technology of Japan (18591170); Nihon University Research Grant for 2008.

#### CONFLICT OF INTEREST

None declared.

#### REFERENCES

- Kaufman, S. and Fisher, D.B. (1974) Pterin-requiring aromatic amino acid hydroxylases in *Molecular mechanisms of oxygen activation* (Hayaishi, O., ed.), pp. 285–370, Academic Press, New York
- Kaufman, S. (1997) Basic Biochemistry and Role in Human Disease in *Tetrahydrobiopterin*. pp. 30–234, The Johns Hopkins University Press, Baltimore
- Kwon, N.S., Nathan, C.F., and Stuehr, D.J. (1989) Reduced biopterin as a cofactor in the generation of nitrogen oxides by murine macrophages. *J. Biol. Chem.* **264**, 20496–20501
- Tayeh, M.A. and Marletta, M.A. (1989) Macrophage oxidation of L-arginine to nitric oxide, nitrite and nitrate. Tetrahydrobiopterin is required as a cofactor. *J. Biol. Chem.* **264**, 19654–19658
- Switchenko, A.C., Primus, J.P., and Brown, G.M. (1984) Intermediates in the enzymic synthesis of tetrahydrobiopterin in *Drosophila melanogaster*. *Biochem. Biophys. Res. Commun.* **120**, 754–760
- Milstien, S. and Kaufman, S. (1985) Biosynthesis of tetrahydrobiopterin: Conversion of dihydroneopterin triphosphate to tetrahydropterin intermediates. *Biochem. Biophys. Res. Commun.* **128**, 1099–1107
- Milstien, S. and Kaufman, S. (1989) Immunological studies on the participation of 6-pyruvoyl tetrahydropterin (2'-oxo) reductase, an aldose reductase, in tetrahydrobiopterin biosynthesis. *Biochem. Biophys. Res. Commun.* **165**, 845–850
- Bonafé, L., Thöny, B., Penzien, J.M., Czarnecki, B., and Blau, N. (2001) Mutations in the sepiapterin reductase gene cause a novel tetrahydropterin dependent monoamine neurotransmitter deficiency without hyperphenylalaninemia. *Am. J. Hum. Genet.* **69**, 269–277
- Blau, N., Bonafé, L., and Thöny, B. (2001) Tetrahydrobiopterin deficiencies without hyperphenylalaninemia: diagnosis and genetics of dopa-responsive dystonia and sepiapterin reductase deficiency. *Mol. Gen. Metab.* **74**, 172–185
- Elzaouk, L., Osmani, H., Leimbacher, W., Romstad, A., Friedman, J., Maccollin, M., Thöny, B., and Blau, N. (2002) *Sepiapterin reductase deficiency: molecular analysis in a new case presenting with neurotransmitter deficiency without hyperphenylalaninemia in Chemistry and Biology of Pteridine and Folates*. (Milstien, S., Kapatos, G., Shane, B., and Levine, R.A., eds.) pp. 277–285, Kluwer Academic Publishers, Norwell
- Park, Y.S., Heizmann, C.W., Wermuth, B., Levine, R.A., Steinerstauch, P., Guzman, J., and Blau, N. (1991) Human carbonyl and aldose reductase: new catalytic functions in tetrahydrobiopterin biosynthesis. *Biochem. Biophys. Res. Commun.* **175**, 738–744
- Iino, T., Sawada, H., Tsusue, M., and Takikawa, S. (1996) Discovery of a new tetrahydrobiopterin-synthesizing enzyme in the lemon mutant of the silkworm *Bombyx mori*. *Biochim. Biophys. Acta.* **1297**, 191–199
- Iino, T., Itoh, N., Sawada, H., Takikawa, S., and Yamamoto, T. (1997) Occurrence of a tetrahydrobiopterin synthesizing enzyme distinct from sepiapterin reductase from normal strain of the silkworm, *Bombyx mori*. *J. Seric. Sci. Jpn* **66**, 439–444
- Iino, T., Takikawa, S., Yamamoto, T., and Sawada, H. (2000) The enzyme that synthesizes tetrahydrobiopterin from 6-pyruvoyl-tetrahydropterin in the lemon mutant silkworm consists of two carbonyl reductases. *Arch. Biochem. Biophys.* **373**, 442–446
- Iino, T., Tabata, M., Takikawa, S., Sawada, H., Shintaku, H., Ishikura, S., and Hara, A. (2003) Tetrahydrobiopterin is synthesized from 6-pyruvoyl-tetrahydropterin by the human aldo-keto reductase AKR1 family members. *Arch. Biochem. Biophys.* **416**, 180–187
- Yang, S., Lee, Y.J., Kim, J.M., Park, S., Peris, J., Laipis, P., Park, Y.S., Chung, J.H., and Oh, S.P. (2006) A murine model for human sepiapterin-reductase deficiency. *Am. J. Hum. Genet.* **78**, 575–587
- Takazawa, C., Fujimoto, K., Homma, D., Chiho, Sumi-Ichinose, Nomura, T., Ichinose, H., and Katoh, S. (2008) A brain-specific decrease of the tyrosine hydroxylase protein in sepiapterin reductase-null mice-as a mouse model for

- Parkinson's disease. *Biochim. Biophys. Res. Comm.* **367**, 787-792
18. Yoshioka, S., Masada, M., Yoshida, T., Inoue, K., Mizokami, T., and Akino, M. (1983) Synthesis of biopterin from dihydroneopterin triphosphate by rat tissues. *Biochim. Biophys. Acta* **756**, 276-285
  19. Fukushima, K., Richter, W.E., and Shiota, T. (1977) Partial purification of 6-(D-erythro-1',2',3'-trihydroxypropyl)-7,8-dihydropterin triphosphate synthetase from chicken liver. *J. Biol. Chem.* **252**, 5750-5755
  20. Takikawa, S., Curtius, H.-Ch., Redweik, U., Leimbacher, W., and Ghisla, S. (1986) Biosynthesis of tetrahydrobiopterin, purification and characterization of 6-pyruvoyl-tetrahydropterin synthase from human liver. *Eur. J. Biochem.* **161**, 295-302
  21. Matsuura, K., Shiraishi, H., Hara, A., Sato, K., Deyashiki, Y., Ninomiya, M., and Sakai, S. (1998) Identification of a principal mRNA species for human 3-hydroxysteroid dehydrogenase isoform (AKR1C3) that exhibits high prostaglandin D2 11-ketoreductase activity. *J. Biochem.* **124**, 940-946
  22. Sato, K., Inazu, A., Yamaguchi, S., Nakayama, T., Deyashiki, Y., Sawada, H., and Hara, A. (1993) Monkey 3-deoxyglucosone reductase: Tissue distribution and purification of three multiple forms of the kidney enzyme that are identical with dihydrodiol dehydrogenase, aldehyde reductase, and aldose reductase. *Arch. Biochem. Biophys.* **307**, 286-294
  23. Fukushima, K. and Nixon, J.C. (1980) Analysis of reduced forms of biopterin in biological tissues and fluids. *Anal. Biochem.* **102**, 176-188
  24. Lin, H.-K., Steckelbroeck, S., Fung, K.-M., Jones, A.N., and Penning, T.M. (2004) Characterization of a monoclonal antibody for human aldo-keto reductase AKR1C3 (type 2 3 $\alpha$ -hydroxysteroid dehydrogenase/type 5 17 $\beta$ -hydroxysteroid dehydrogenase): immunohistochemical detection in breast and prostate. *Steroids* **69**, 795-801
  25. Graham, A., Brown, L., Hedge, P.J., Gammack, A.J., and Markham, A.F. (1991) Structure of the human aldose reductase gene. *J. Biol. Chem.* **266**, 6872-6877
  26. Sawada, H., Shimura, N., Takikawa, S., and Iino, T. (2005) Possibility of the nonenzymatic conversion of 6-(1'-oxo-2'-hydroxypropyl)-tetrahydropterin to sepiapterin. *Pteridines* **16**, 11-14
  27. Penning, T.M., Burczynski, M.E., Jez, J.M., Hung, C.-F., Lin, H.-K., Haiching, M.A., Moore, M., Palackal, N., and Ratnam, K. (2000) Human 3 $\alpha$ -hydroxysteroid dehydrogenase isoforms (AKR1C1-AKR1C4) of the aldo-keto reductase superfamily: functional plasticity and tissue distribution reveals roles in the inactivation and formation of male and female sex hormones. *Biochem. J.* **351**, 67-77

# Urinary metabolic profile of phenylketonuria in patients receiving total parenteral nutrition and medication

Tomiko Kuhara<sup>1\*</sup>, Morimasa Ohse<sup>1</sup>, Yoshito Inoue<sup>1</sup>, Toshihiro Shinka<sup>1</sup>, Yoshiyuki Okano<sup>2</sup>, Haruo Shintaku<sup>2</sup>, Kazuhisa Hongou<sup>3</sup>, Toshio Miyawaki<sup>3</sup>, Wakaba Morinobu<sup>4</sup>, Hiroshi Tamai<sup>4</sup> and Kenji Omura<sup>5</sup>

<sup>1</sup>Division of Human Genetics, Medical Research Institute, Kanazawa Medical University, Uchinada, Ishikawa 920-0293, Japan

<sup>2</sup>Department of Pediatrics, Osaka City University School of Medicine, Asahimachi, Abeno-ku, Osaka 545-8585, Japan

<sup>3</sup>Department of Pediatrics, Toyama Medical and Pharmaceutical University, Sugitani, Toyama 930-0194, Japan

<sup>4</sup>Department of Pediatrics, Osaka Medical College, Takatsuki, Osaka 569-8686, Japan

<sup>5</sup>Department of General and Cardiothoracic Surgery, Kanazawa University School of Medicine, Takara-machi, Kanazawa 920-8640, Japan

Received 28 April 2009; Revised 16 July 2009; Accepted 2 August 2009

Nutrition and drugs are main environmental factors that affect metabolism. We performed metabolomics of urine from an 8-year-old patient (case 1) with epilepsy and an 11-year-old patient (case 2) with malignant lymphoma who was being treated with methotrexate. Both patients were receiving total parenteral nutrition (TPN). We used our diagnostic procedure consisting of urease pretreatment, partial adoption of stable isotope dilution, gas chromatography/mass spectrometry (GC/MS) measurement and target analysis for 200 analytes including organic acids and amino acids. Surprisingly, their metabolic profiles were identical to that of phenylketonuria. The neopterin level was markedly above normal in case 1, and both neopterin and biopterin were significantly above normal in case 2. Mutation analysis of genomic DNA from case 1 showed neither homozygosity nor heterozygosity for phenylalanine hydroxylase deficiency. The metabolic profiles of both cases were normal when they were not receiving TPN. TPN is presently prohibited for individuals who have inherited disorders that affect amino acid metabolism. Although the Phe content of the TPN was not the sole cause of the PKU profile, its effect, combined with other factors, e.g. specific medication or possibly underlying diseases, led to this metabolic abnormality. The present study suggests that GC/MS-based metabolomics by target analysis could be important for assuring the safety of the treatments for patients receiving both TPN and methotrexate. Metabolomic profiling, both before and during TPN, is useful for determining the optimal nutritional formula not only for neonates, but also for young children who are known heterozygotes for metabolic disorders or whose status is unknown. Copyright © 2009 John Wiley & Sons, Ltd.

Total parenteral nutrition (TPN) is given to patients whose digestive system has been impaired for more than 2 weeks. It provides amino acids directly into a systemic vein, as a source of nitrogen. The amino acid formula follows the recommendation of the Food and Agricultural Organization/World Health Organization (FAO/WHO), which is based on the content of mature human milk. It is generally expected that, in patients on TPN, the blood amino acid level will not exceed twice the control level, and the urinary amino acid profile will be normal. TPN is presently prohibited for individuals who are known to have inherited disorders relating to the metabolism of amino acids but not for those whose status is unknown or who are heterozygous for these disorders. Examination of patient samples by metabolomic screening before beginning TPN could be important for the safety of patients whose status for metabolic disorders is

unknown, and could likewise be valuable for heterozygotes for metabolic disorders, both before and during TPN. We have developed a method for noninvasive metabolic profiling using urine samples to measure various classes of compounds including amino acids and organic acids, simultaneously, and we began to use this method to design personalized medicine for patients with inborn errors of metabolism in 1996.<sup>1</sup> This method has allowed us to make chemical diagnoses of many cases of inborn errors of metabolism, including phenylketonuria (PKU) in a single gas chromatography/mass spectrometry (GC/MS) run.

The major metabolic pathway for Phe is hydroxylation to yield tyrosine (Fig. 1). Hyperphenylalaninemia is caused by Phe hydroxylase (PAH) deficiency, reduced supply of tetrahydrobiopterine (BH<sub>4</sub>), a cofactor for PAH, or impaired regeneration of the BH<sub>4</sub>. In PKU, due to severe hyperphenylalaninemia, Phe is metabolized via a by-path to phenylpyruvate, 2-hydroxyphenylacetate, phenyllactate and phenylacetate. The levels of these aromatic acids, however, do not increase measurably in mild

\*Correspondence to: T. Kuhara, Division of Human Genetics, Medical Research Institute, Kanazawa Medical University, Daigaku, Uchinada, Kahoku-gun, Ishikawa 920-0293, Japan.  
E-mail: kuhara@kanazawa-med.ac.jp



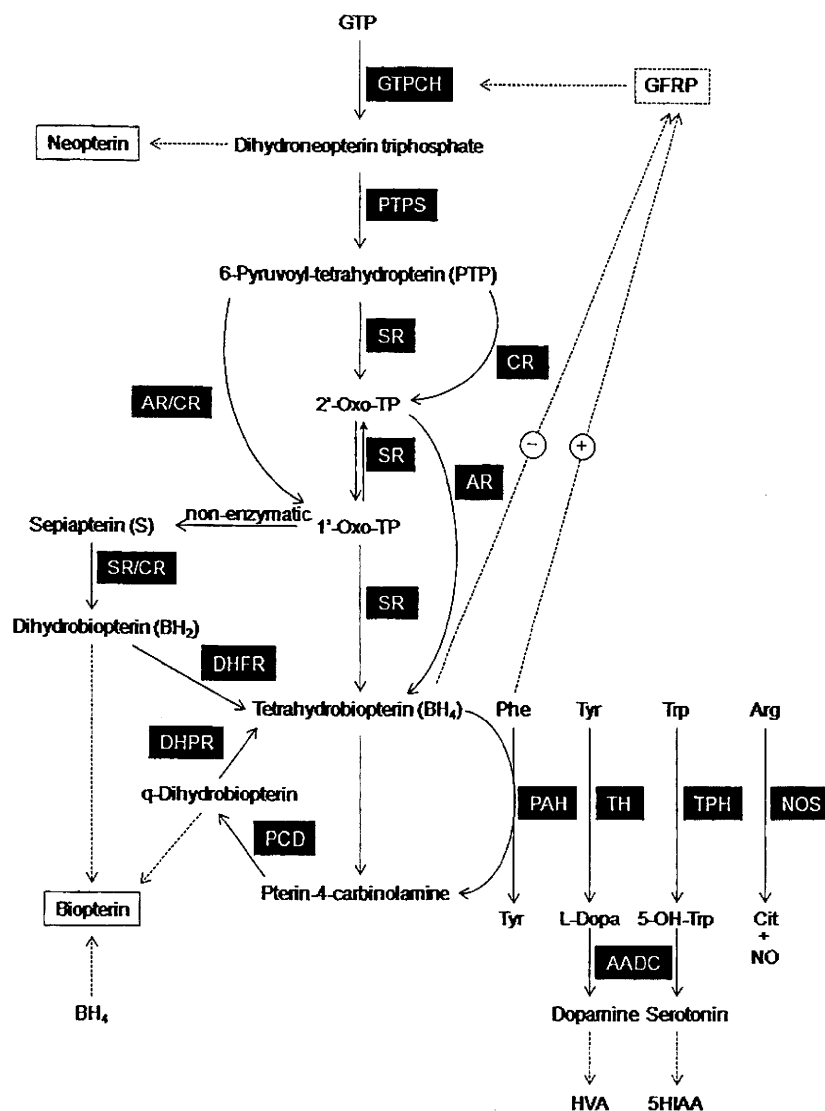


**Figure 1.** Biosynthesis and recycling of tetrahydrobiopterin. GTPCH, GTP cyclohydrolase I; PTPS, 6-pyruvoyl tetrahydropterin synthase I; SR, sepiapterin reductase; CR, carbonyl reductase; AR, aldose reductase; DHFR, dihydrofolate reductase; GTP, guanosine triphosphate; 1'-oxo-TP, 1'-oxo-2'-hydroxytetrahydropterin (6-lactoyl tetrahydropterin); 2'-oxo-TP, 1'-hydroxy-2'-oxotetrahydropterin; GFRP, GTP cyclohydrolase I feedback regulatory protein; DHPR, dihydropteridin reductase; PCD, pterin-4-carbinolamine dehydratase; PAH, phenylalanine-4-hydroxylase; TH, tyrosine-3-hydroxylase; TPH, tryptophan-5-hydroxylase; 5-OH-Trp, 5-hydroxytryptophan; NO, nitric oxide; NOS, nitric oxide synthase; AADC, aromatic amino acid decarboxylase; HVA, homovanillic acid; 5-HIAA, 5-hydroxyindoleacetic acid.

hyperphenylalaninemia or biopterin-responsive hyperphenylalaninemia.<sup>2,3</sup>

Nutrition and drugs are the main environmental factors that affect metabolism. We found that the metabolic profiles of two patients undergoing TPN were identical with that for PKU, even though these patients did not have PKU and were being treated with different medications. This report describes severe hyperphenylalaninemia during TPN and other factors that may have contributed to this metabolic change.

## EXPERIMENTAL

### Patients

#### Case 1

A 4-year-old boy was admitted to the hospital with epilepsy accompanied by pneumonia. Ten months after birth, he had suffered his first seizure. After that, numerous examinations, including a muscle biopsy, had been performed. However, no definite diagnosis had been made. The histopathological findings of the muscle-biopsy specimen suggested myogenic

disease. The boy had spastic palsy of the extremities accompanied by severe mental retardation.

During this hospital stay, hyperammonemia was noted. A first urine metabolic profiling was conducted based on suspicion of a disturbed amino acid metabolism. The presence of primary and secondary hyperammonemia and other metabolic disorders was ruled out, and the Guthrie blood test done when this patient was a neonate was negative for hyperphenylalaninemia. During this hospitalization, the frequency of the patient's seizures decreased as the infection subsided.

At the age of eight, the frequency of seizures increased again, accompanied by convulsions every few minutes, and the boy was hospitalized. Anesthesia with continuous thiopental drip infusion was attempted to relieve the seizures for 3 days. Because oral intake was impossible, and the risk of aspiration was high, nutritional therapy with TPN containing 2.3 g/L of Phe was initiated, at a rate of 50 mL/h. Brain computer tomography showed brain atrophy, probably due to the continuous thiopental administration. A second urine metabolic profile was conducted. Later, an arachnoid cystectomy was carried out, which alleviated the seizures. Since then, the boy has been staying at another hospital and receiving respiratory management, physical therapy, and other appropriate care. The boy's parents gave their informed consent for us to perform a mutational analysis of the boy's PAH gene.

#### Case 2

An 11-year-old boy was admitted to the hospital with a subcutaneous mass of the head. His family history was unremarkable. After closer examination, he was given a diagnosis of non-Hodgkin's lymphoma, lymphoblastic type, stage IV. In April of the same year, first-line chemotherapy using methotrexate, vincristine, adriamycin, and prednisolone was started. During the chemotherapy, the patient suffered from severe gastrointestinal toxicity, including nausea and vomiting. TPN was necessary to supply an adequate amount of nutrition. His condition was complicated by steroid-induced diabetes mellitus and renal stones. Insulin therapy was necessary to control his hyperglycemia. To rule out a metabolic disorder, a first metabolic profiling of urine collected during TPN was conducted. At that time, no anti-tumor agent was being used. However, 2 weeks before the sampling, the patient had received high-dose methotrexate therapy.

Two months later, second-line chemotherapy with cyclophosphamide, daunomycin, vincristine, prednisolone, and L-asparaginase was introduced. As the patient's oral intake was much improved, no parenteral nutrition was needed. A second urinary metabolic profiling was conducted during the second-line chemotherapy. Although the boy responded to the second-line chemotherapy, he had repeated cycles of remission and relapse. The patient died of the underlying disease 1 year later.

#### Materials and methods

The amount of creatinine and creatine in urine was determined on a Beckman CX5 autoanalyzer. The preparation of urine, including the pretreatment with urease and

ethanol deproteinization to remove the urease, partial adoption of a stable isotope dilution, trimethylsilylation, and capillary GC/MS analysis were as described.<sup>1,4</sup> A volume of 100  $\mu$ L of urine was pretreated with type C-3 urease at 37°C for 10 min to decompose and remove excess urea. For quantification, the urine was spiked with fixed amounts of internal standards: 20 nmol each of 2,2-dimethylsuccinate and 2-hydroxyundecanoate; 100 nmol of [<sup>2</sup>H<sub>3</sub>]creatinine; 4 nmol of [<sup>15</sup>N<sub>2</sub>]uracil and [<sup>15</sup>N<sub>2</sub>]orotate; 10 nmol of [<sup>2</sup>H<sub>3</sub>]methionine, [<sup>2</sup>H<sub>3</sub>]homocystine, [<sup>2</sup>H<sub>4</sub>]cystine, [<sup>2</sup>H<sub>3</sub>]leucine, [<sup>2</sup>H<sub>5</sub>]phenylalanine and [<sup>2</sup>H<sub>4</sub>]tyrosine; 5 nmol of [<sup>2</sup>H<sub>3</sub>]methylcitrate; and 50 nmol [<sup>2</sup>H<sub>5</sub>]glycine and [<sup>2</sup>H<sub>4</sub>]lysine.

Aliquots (0.2 or 1  $\mu$ L) of the derivatized extracts were injected into a Hewlett-Packard GC-MSD (HP6890/MSD5973) equipped with a fused-silica DB-5 capillary column (30 m  $\times$  0.25 mm i.d. with a 0.25  $\mu$ m film thickness; J&W, Folsom, CA, USA) with a split ratio of 1:10 to 1:50. Electron impact mass spectra were obtained at a scan rate of 2.5 cycles/s from *m/z* 50 to 650.

Two hundred components, from lactate to homocystine, were automatically identified, quantified, or semi-quantified.<sup>5</sup> The levels of most metabolites for age-matched healthy individuals are not normally distributed. Therefore, they were log<sub>10</sub>-transformed, and the mean and standard deviation (SD) were obtained. For the evaluation of a metabolite in the urine of the patients, an abnormality *n* was defined as *n* in [mean value of age-matched control above *n*  $\times$  SD], which was obtained automatically.<sup>5</sup>

#### RESULTS AND DISCUSSION

Analysis of urine metabolome obtained by single 15 min GC/MS measurement enabled detection of the metabolic disorder caused secondarily. A metabolic profile identical with PKU was found for two patients undergoing TPN with 2.3 g/L Phe: an 8-year-old boy under general anesthesia with thiopental, a p-450 inducer, for the control of convulsions (case 1) and an 11-year-old boy with malignant lymphoma receiving methotrexate treatment (case 2). The total ion current (TIC) chromatogram of the trimethylsilyl (TMS) derivatives of metabolites in the first urine sample from case 2 is shown in Fig. 2. A target analysis of more than 200 analytes including amino acids, organic acids, alcohol, sugars, sugar acids, purine and pyrimidine was performed using the intensity of ions of a specific *m/z* at a specific retention time, and the abnormality *n* in [mean above *n*  $\times$  SD] for the metabolites was calculated automatically.<sup>5</sup> As shown in Table 1, the abnormality of Phe, phenyllactate, 2-hydroxyphenylacetate and phenylacetate was 5.7, 10.2, 7.0 and 4.6, respectively, in case 1, and 7.8, 10.5, 4.9 and 5.7, in case 2. The serum Phe was increased in case 1, and plasma Phe estimated from that in the urine according to Boulos *et al.*<sup>6</sup> was high in both cases. These data indicated that both patients had a metabolic profile identical with PKU. In general, a low Phe diet is recommended to prevent the pathogenesis associated with hyperphenylalaninemia, in classic PKU (higher than 1.2 mM), mild PKU (higher than 0.72 mM), and hyperphenylalaninemia (higher than 0.4 mM), to maintain the blood Phe level below 0.4 mM.<sup>7</sup> When the

**Table 2.** Relationship between the pteridine profile, the PKU profile, and TPN

Case	Age at urine sampling	Neopterin	Biopterin	N/B ratio	PKU profile	TPN
Case 1						
1st	4Y10M	2.35	1.09	2.16	-	-
2nd	8Y3M	38.08	1.13	33.72	+	+
Case 2						
1st	11Y	4.45	6.05	0.74	+	+
2nd	11Y2M	0.88	1.58	0.55	-	-
Control	5-10Y	0.59 ± 0.29	1.31 ± 0.58	0.5 ± 0.2	-	-
	10-16Y	0.43 ± 0.25	0.96 ± 0.41	0.5 ± 0.1	-	-

Values for pteridine are expressed as mmol/mol creatinine. Y, year; M, month.

The 1st and 2nd analyses for both cases were of the same urine specimens used for the metabolic profiling shown in Table 1.

disorders characterized by hyperphenylalaninemia and a deficiency of monoamine neurotransmitters. BH4 deficiency is caused by mutations in the genes encoding six enzymes responsible for BH4 biosynthesis and regeneration.<sup>10</sup>

In contrast to classical forms of BH4 deficiency, two others, DOPA-responsive dystonia, caused by autosomal dominant mutations in the GTP cyclohydrolase I gene, and sepiapterin reductase deficiency, an autosomal recessive disease, do not present with hyperphenylalaninemia and thus cannot be detected by neonatal screening for PKU.<sup>11</sup> Phe loading, however, can unmask these disorders by causing hyperphenylalaninemia. The amount of Phe supplied by TPN per day corresponds to that used in the standard Phe loading test. Neonates on TPN can show transient PKU profiles,<sup>12</sup> but older patients usually do not, unless there is additional underlying factor at play. Patients with DOPA-responsive dystonia or sepiapterin reductase deficiency, however, have such a factor, and have a high risk of developing hyperphenylalaninemia during TPN.

The concentrations of neopterin and biopterin in the present cases were determined by a method reported previously<sup>13</sup> and are shown in Table 2. Neither patient had dystonia nor a low neopterin level (Table 2). BH4 biosynthesis is stimulated by Phe and suppressed by BH4. The metabolic profiles taken when the patients were off TPN showed a normal pterin profile in case 2 and a normal biopterin profile in case 1, with a slight increase in neopterin that might have been caused by the infectious pneumonia. When the patients were on TPN, the metabolic profile in case 2 showed significantly increased neopterin and biopterin, with a normal neopterin/biopterin ratio, and that in case 1 showed markedly increased neopterin with a very high neopterin/biopterin ratio. This marked increase in neopterin also indicated that GTP cyclohydrolase I was not defective in case 1.

Recent studies on BH4 uptake demonstrate that the liver can take up BH4 only indirectly, via a pathway involving prior oxidation and dihydrofolate reductase reaction, and that BH4 deposition in the liver is completely inhibited by prior treatment with methotrexate, a folate analogue and dihydrofolate reductase inhibitor.<sup>14,15</sup> Methotrexate also inhibits the PAH system by preventing the regeneration of BH4 as a dihydropteridine reductase inhibitor.<sup>16,17</sup> Hyperphenylalaninemia and acute or subacute neurological disorders have been occasionally reported in patients receiving high-dose methotrexate therapy.<sup>16,18</sup> Although a

large amount of folinic acid was administered after methotrexate chemotherapy to rescue the tetrahydrofolate and folate metabolism, this treatment may not rescue the BH4 metabolism.

In the urine from case 2 during TPN and after methotrexate chemotherapy, an unknown metabolite was detected having GC retention time of 13.455 min. The highest mass was detected at *m/z* 525 and the base peak at *m/z* 409 [M-116]. Ions at *m/z* 73, 117, 147, 408 [M-117] and 510 [M-15] are found suggesting biopterin-4TMS. The mass spectrum and the retention time were identical with those of authentic biopterin. The presence of biopterin suggested that *q*-dihydrobiopterin, the substrate for dihydropteridine reductase, was increased. It was, however, suggested that for the quantitative evaluation of these pterins using GC/MS, analysis at higher column temperature should be performed. Two other unknown peaks are under structural elucidation.

In general, the severity of the adverse effects caused by metabolic mimics of PKU may depend on the age of the patients and the duration of the metabolic profile. TPN was used for only a short time in the present cases, and the PKU profile cannot be attributed solely to the TPN. The time difference between the end of the infusion and the collection of the urine specimens was not recorded for either case. It is not clear, therefore, whether the PKU profiles we observed were representative, or if the profile was at times more severe. Nevertheless, the present study suggests that urine metabolic profiling is useful for understanding the metabolic state of patients receiving TPN during various medical treatments. It is important to determine the optimal nutritional formula, not only for neonates but also for younger children who undergo methotrexate chemotherapy, especially when TPN must be provided for a long period of time. If a PKU profile is detected during methotrexate chemotherapy, the administration of BH4 or lowering of the Phe content in the TPN may be effective.

## CONCLUSIONS

We found that two patients had metabolic profiles characteristic of PKU while receiving TPN, but normal profiles without TPN. Although the marginally high Phe content of the TPN was almost certainly not the sole cause of these results except for neonates, its effect, combined with other factors including genetic factors and drugs such as methotrexate, led to the PKU profile. Targeted analysis of

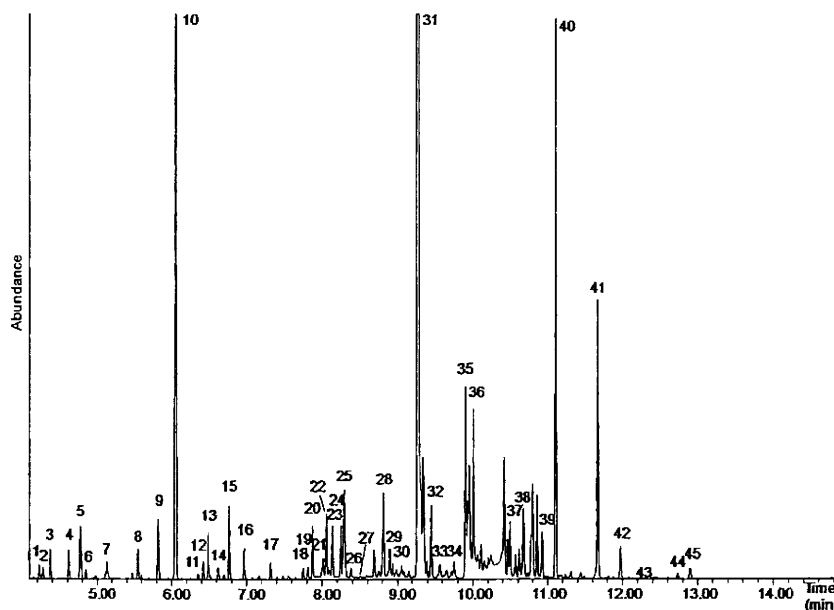


**Figure 2.** TIC chromatogram of trimethylsilyl derivatives of metabolites from urine (case 2). Major component of each major peak: 1, lactate-2; 2, 2-hydroxyisobutyrate-2; 3, glycolate-2; 4, alanine-2; 5, glycine-2; 6, oxalate-2; 7, sulfate-2; 8,  $\beta$ -aminoisobutyrate-2; 9, urea-2; 10, phosphate-3; 11, phenylacetate-1; 12, succinate-2; 13, 2,2-dimethylsuccinate-2 (IS); 14, N2-uracil-2 (IS); 15, serine-3; 16, threonine-3; 17, 2-deoxytetronate-3; 18, malate-3; 19, threitol-4; 20, erythritol-4; 21, D3-methionine-2 (IS); 22, 5-oxoproline-2; 23, threonate-4; 24, erythronate-4; 25, creatinine-3; 26, 2-hydroxyphenylacetate-2; 27, phenyllactate-2; 28, phenylalanine-2; 29, 4-hydroxyphenylacetate-2; 30, asparagine-3; 31, xylitol-5; 32, 2-hydroxyundecanoate-2 (IS); 33, cis-aconitate-3; 34, glutamine-3; 35, fructose-5; 36, citrate-4; 37, gluconate-4; 38, histidine-3; 39, glucose-5; 40, gluconate-6; 41, urate-4; 42, heptadecanoate-1 (IS); 43, tryptophan-3; 44; D4-cystine-4 (IS); 45, pseudouridine-5.

patients were off TPN, these metabolite levels were normal or significantly lower: in case 1, only a very mild amino aciduria was present; and, in case 2, tyrosine and methionine were increased (Table 1).

The incidence of PKU and PAH heterozygotes is 1/70 000 and 1/130, respectively, in Japan. In case 1, 13 exons of the PAH gene and its flanking intronic regions were screened using denaturing high-performance liquid chromatography

(HPLC),<sup>8</sup> and exons 7 and 12 were sequenced as described.<sup>9</sup> No mutations were found except for a V245V silent mutation in exon 7; thus, it was unlikely that this patient was heterozygous for a PAH deficiency. Because of the patient's early death in case 2, we could not perform a mutation analysis for PAH.

BH4 is an essential cofactor for PAH and other enzymes, as shown in Fig. 1. BH4 deficiency causes severe neurological

**Table 1.** Abnormality  $n$  of metabolites and Phe concentrations

Analysis	Abnormality $n$ of metabolites in urine								Phe conc.		
	Phe <sup>a</sup>	2HPA <sup>b</sup>	PL <sup>c</sup>	PA <sup>d</sup>	Tyr <sup>e</sup>	Trp <sup>f</sup>	Met <sup>g</sup>	Gluc <sup>h</sup>	Urine <sup>i</sup>	Plasma <sup>j</sup> (mM)	Serum <sup>k</sup> (mM)
Case 1											
1st	0.9	2.2	-0.7	1.7	0.9	-1.1	-2.7	2.0	14	0.09	
2nd	5.7	10.2	7.0	4.6	1.0	-0.5	6.5	3.3	124	1.10	0.72
Case 2											
1st	7.8	10.5	4.9	5.7	2.4	3.0	2.6	2.3	310	2.67	
2nd	4.8	3.5	3.7	1.6	5.2	3.0	5.1	<10.0	81	0.73	

The levels of 2-hydroxyphenylacetate, phenylacetate, and phenyllactate were obtained relative to the internal standard, 2,2-dimethylsuccinate, and amino acids, by stable isotope dilution. The levels of urinary metabolites in age-matched healthy individuals were  $\log_{10}$ -transformed, and the mean and SD were obtained. The abnormality  $n$  in [mean above  $n \times SD$ ] is shown for metabolites, <sup>a</sup>phenylalanine, <sup>b</sup>2-hydroxyphenylacetate, <sup>c</sup>phenyllactate, <sup>d</sup>phenylacetate, <sup>e</sup>tyrosine, <sup>f</sup>tryptophan, <sup>g</sup>methionine, and <sup>h</sup>glucose, at the 1st and 2nd metabolic profiling. <sup>i</sup>Urine Phe concentrations are expressed as mmol/mol creatinine. <sup>j</sup>Plasma concentration was estimated from that in urine according to Boulos *et al.*<sup>6</sup> <sup>k</sup>Serum concentration was determined in case 1, for which serum was obtained.

the GC/MS-based urine metabolome including amino acids and organic acids, obtained in a single run, enables rapid understanding of the metabolic state of the patients under TPN with medication. This highly sensitive and specific GC/MS-based metabolomics is an essential approach for global personalized medicine.

### Acknowledgements

The authors wish to acknowledge Dr. N. Takizawa, National Sanatorium Toyama Hospital Japan, for his help in this study.

### REFERENCES

1. Matsumoto I, Kuhara T. *Mass Spectrom. Rev.* 1996; **15**: 43.
2. Blau N, Thöny B, Cotton RGH, Hyland K. In *The Metabolic and Molecular Bases of Inherited Diseases*, (8th edn) Scriver CR, Beaudet AL, Sly WS, Valle D (eds). McGraw-Hill: New York, 2001; 1725–1776.
3. Scriver CR, Kaufman S. In *The Metabolic and Molecular Bases of Inherited Diseases*, (8th edn) Scriver CR, Beaudet AL, Sly WS, Valle D (eds). McGraw-Hill: New York, 2001; 1667–1724.
4. Kuhara T. *J. Chromatogr. B.* 2001; **758**: 3.
5. Kuhara T. *Mass Spectrom. Rev.* 2005; **24**: 814.
6. Boulos M, Boulat O, Van Melle G, Guignard JP, Matthieu J. *Biol. Neonate* 2004; **86**: 6.
7. Costello PM, Beasley MG, Tillotson SL, Smith I. *Eur. J. Pediatr.* 1994; **153**: 260.
8. Okano Y, Asada M, Kang Y, Nishi Y, Hase Y, Oura T, Isshiki G. *Hum. Genet.* 1998; **103**: 613.
9. Brautigam S, Kujat A, Kirst P, Seidel J, Luleyap HU, Froster UG. *Mol. Genet. Metab.* 2003; **78**: 205.
10. Blau N, Bonafé L, Thöny B. *Mol. Genet. Metab.* 2001; **74**: 172.
11. Bonafé L, Thöny B, Leimbacher W, Kierat L, Blau N. *Clin. Chem.* 2001; **47**: 477.
12. Evans SJ, Wynne-Williams TC, Russell CA, Fairbrother A. *Lancet* 1986; **ii**: 1404.
13. Shintaku H, Niederwieser A, Leimbacher W, Curtius HC. *Eur. J. Pediatr.* 1988; **147**: 15.
14. Sawabe K, Suetake Y, Nakanishi N, Wakasugi K, Hasegawa H. *Mol. Genet. Metab.* 2005; **86** (Suppl 1): S133.
15. Sawabe K, Suetake Y, Wakasugi K, Hasegawa H. *Mol. Genet. Metab.* 2005; **86** (Suppl 1): S145.
16. Millot F, Dhondt JL, Hayte JM, Bauters F. *Am. J. Pediatr. Hematol. Oncol.* 1992; **14**: 276.
17. Millot F, Dhondt JL, Mazingue F, Mechinaud F, Ingrand P, Guilhot F. *Pediatr. Res.* 1995; **37**: 151.
18. Blau N, Curtius AC, Kierat L, Leupold D, Kohne E. *J. Pediatr.* 1989; **115**: 661.

## Letters to the Editor Related to New Topics

### Plasma Phenylalanine Level in Dopa-Responsive Dystonia

DYT5 is a condition characterized by levodopa (L-dopa) responsive dystonia (DRD) that shows childhood onset and marked diurnal fluctuation. Patients with DYT5 have heterozygous mutations in the GCH1 gene, which codes for GTP cyclohydrolase I (GTPCH), a rate-limiting enzyme in tetrahydrobiopterin (BH<sub>4</sub>) synthesis.<sup>1</sup> BH<sub>4</sub> is a cofactor for aromatic amino acid hydroxylases including tyrosine hydroxylase (TH), phenylalanine hydroxylase (PAH), and tryptophan hydroxylase.<sup>2</sup> In patients with DYT5, production of dopamine is suppressed due to the decrease of BH<sub>4</sub> because TH is a rate-limiting enzyme in dopamine synthesis. The lack of BH<sub>4</sub> may also affect the activity of PAH, and patients with complete GTPCH deficiency show hyperphenylalaninemia. However, hyperphenylalaninemia has not been reported in patients with DYT5.<sup>3</sup> Therefore, we examined blood phenylalanine levels in patients with DYT5 compared with controls to determine whether the decrease of BH<sub>4</sub> in DYT5 affects PAH activity.

Blood samples for analysis of amino acids were obtained from seven patients with DRD<sup>4</sup> and heterozygous mutations of GCH1, 24 patients with dopa nonresponsive dystonia (non-DRD), and 12 controls. The samples were collected in a tube containing EDTA, and plasma was obtained for analysis of phenylalanine and tyrosine levels using an auto-amino acid analyzer (HS-3000; Hitachi, Tokyo, Japan). All data are expressed as means  $\pm$  SD. The data were analyzed by analysis of variance (ANOVA) with multiple comparison using the Bonferroni method. A significant difference was defined as a *P* value  $<$  0.05.

The phenylalanine and tyrosine levels in the plasma of patients with DYT5, patients with non-DRD, and controls are shown in Figure 1. The phenylalanine levels in the DYT5 ( $81.1 \pm 26.6 \mu\text{mol/L}$ ), non-DRD ( $60.5 \pm 14.5 \mu\text{mol/L}$ ), and control ( $58.7 \pm 9.1 \mu\text{mol/L}$ ) groups were all within the normal range. However, the phenylalanine level in patients with DYT5 was significantly higher than those in the other groups (*P* = 0.027 by ANOVA). Multiple comparison also indicated that the level of plasma phenylalanine in patients with DYT5 was significantly higher than those in patients with non-DRD (*P* = 0.043) and in controls (*P* = 0.040). There was no significant difference in the plasma phenylalanine levels between

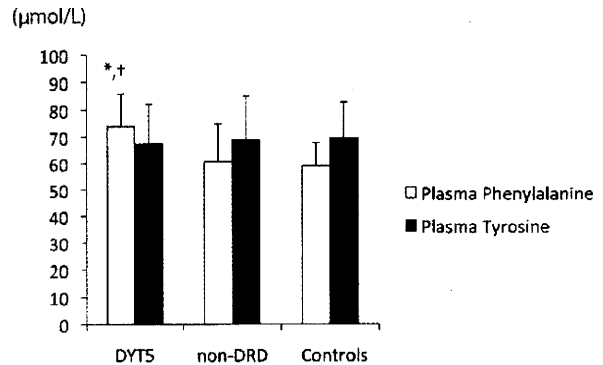


FIG. 1. Plasma phenylalanine and tyrosine levels. The plasma phenylalanine levels (open boxes) and tyrosine levels (closed boxes) are shown for patients with DYT5, patients with non-DRD, and controls. Error bars indicate standard deviations. \**P*  $<$  0.05 (DYT5 vs. non-DRD). †*P*  $<$  0.05 (DYT5 vs. controls).

patients with non-DRD and controls. There were no significant differences in plasma tyrosine levels among all the groups.

BH<sub>4</sub> deficiency causes hyperphenylalaninemia and a decrease of dopamine production, because it suppresses the activity of PAH and TH. Patients with a homozygous mutation in the GCH1 gene are reported to show hyperphenylalaninemia, in addition to DRD. Patients with DYT5 having only a heterozygous mutation in GCH1 also show symptoms of DRD, but do not have hyperphenylalaninemia. Our results indicated that blood phenylalanine levels in patients with DYT5 are within the normal range, but are higher than those in controls, which suggests that the activity of PAH is partially affected by the decrease in BH<sub>4</sub> in DYT5.

GTPCH is regulated by BH<sub>4</sub> itself and phenylalanine via GTPCH feedback regulatory protein (GFRP).<sup>5</sup> An increase of phenylalanine induces GFRP to upregulate GTPCH activity, whereas an increase of BH<sub>4</sub> downregulates GTPCH activity via GFRP. Hyland et al. has reported prolonged hyperphenylalaninemia after oral phenylalanine loading in patients with DRD,<sup>6</sup> which suggests that decreased BH<sub>4</sub> production due to mutations in GTPCH restrict the catalysis of excessive phenylalanine by PAH. However, a defect in GFRP or in the interaction between GTPCH and GFRP would cause the same results. Our results indicate that the phenylalanine level in patients with DYT5 differs from those in controls without phenylalanine loading, which suggests that a partial defect of GTPCH affects the activity of PAH.

**Author Roles:** Hiroki Fujioka, MD, PhD: correcting samples. Performing statistical analysis. Haruo Shintaku, MD: correcting samples, supervising. Satoshi Kudo, PhD: measuring amino acid concentration. Tsunekazu Yamano, MD: supervising.

Potential conflict of interest: Hiroki Fujioka received the Grants-in-Aid for Scientific Research by the Ministry of Education, Culture, Sports, Science and Technology of Japan (No. 20790771). Hiroki Fujioka and Haruo Shintaku received Grants-in-Aid for Scientific Research by the Ministry of Education, Culture, Sports, Science and Technology of Japan (No. 17591109).

Published online 20 October 2009 in Wiley InterScience (www.interscience.wiley.com). DOI: 10.1002/mds.22774

Hiroki Fujioka, MD, PhD\*  
 Haruo Shintaku, MD  
 Satoshi Kudo, PhD  
 Tsunekazu Yamano, MD  
 Department of Pediatrics  
 Osaka City University Graduate School of Medicine  
 Osaka, Japan  
 \*E-mail: hfujioka@msic.med.osaka-cu.ac.jp

Hiroki Fujioka, MD, PhD  
 Osaka City Fukushima-Ward  
 Public Health and Welfare Center  
 Fukushima-Ward Office  
 Osaka, Japan

### References

1. Ichinose H, Ohye T, Takahashi E, et al. Hereditary progressive dystonia with marked diurnal fluctuation caused by mutations in the GTP cyclohydrolase I gene. *Nat Genet* 1994;8:236–242.
2. Shintaku H. Disorders of tetrahydrobiopterin metabolism and their treatment. *Curr Drug Metab* 2002;3:123–131.
3. Blau N, Ichinose H, Nagatsu T, et al. A missense mutation in a patient with guanosine triphosphate cyclohydrolase I deficiency missed in the newborn screening program. *J Pediatr* 1995;126:401–405.
4. Ohta E, Funayama M, Ichinose H, et al. Novel mutations in the guanosine triphosphate cyclohydrolase I gene associated with DYT5 dystonia. *Arch Neurol* 2006;63:1605–1610.
5. Yoneyama T, Hatakeyama K. Decameric GTP-cyclohydrolase I forms complexes with two pentameric GTP cyclohydrolase I feedback regulatory proteins in the presence of phenylalanine or of a combination of tetrahydrobiopterin and GTP. *J Biol Chem* 1998;273:20102–20108.
6. Hyland K, Fryburg JS, Wilson WG, et al. Oral phenylalanine loading in dopa-responsive dystonia: a possible diagnostic test. *Neurology* 1997;48:1290–1297.

### Hybrid Cars May Interfere with Implanted Deep Brain Stimulators

Clinicians and patients are always concerned about potential interference between external electromagnetic fields and implantable pacemaker devices. In a recent *New York Times* article, concern was raised about emitted “magnetic fields” from hybrid cars and association with various diseases such as childhood leukemia.<sup>1</sup> We report a case of a patient with deep brain stimulator placement for Parkinson’s disease who developed unusual symptoms possibly related to stimulator malfunction while riding in a hybrid car.

A 73-year-old man with history of tremor-dominant Parkinson’s disease (PD) underwent bilateral subthalamic nucleus deep brain stimulator (STN DBS) placement. One month later, initial stimulator programming was performed,

and he complained of symptoms of severe nausea, dizziness, and palpitations while driving the 4- to 5-hour journey home in a 2008 hybrid Toyota Prius car. The patient’s wife had to stop the car multiple times as he felt so ill. Prior to initial programming, the patient was able to drive and ride in the Prius without any problems. After stimulator activation, the patient complained of reproducible symptoms of nausea, dizziness, lightheadedness, and cardiac palpitations when sitting in the front passenger seat. He noticed that the symptoms worsened when both the gasoline engine and electric motor were running or when the car battery was charging. The symptoms spontaneously resolved when he exited the car and never occurred when he was in his truck, which is a nonhybrid vehicle. The symptoms also improved when he manually turned off his stimulator while inside the Prius or when he moved to the back seat. These symptoms did not occur at any other time. On interrogation of his stimulator 4 weeks after initial DBS programming, seven activations were noted with only two that were accounted by the patient turning the pulse generator off and on manually. The internal pulse generators (IPGs), however, had been on 99% of the time.

The patient experienced the worst symptoms when sitting in the front seat of the Prius and when the car battery was being charged, suggesting that the electromagnetic field emitted might be interfering with his neurostimulator settings. There were multiple unaccounted activations on interrogation of the stimulator, although the IPGs were on 99% of the time. He did not get symptoms in a nonhybrid car or in the Prius when his IPG was off. We have observed similar symptoms when the voltage of an STN neurostimulator was increased rapidly. We hypothesize that the device was turning off and on rapidly, with voltage surges, thus causing the patient’s symptoms. This is the first documented case of a hybrid vehicle, potentially interfering with the IPG settings in a subject with PD and STN DBS. There has been controversy over the effect of electromagnetic fields generated by hybrid vehicles on cardiac pacemakers and implantable defibrillators. Patients with cardiac pacemakers have complained of similar symptoms as the ones which our patient experienced when inside a hybrid car or near its smart key device (internet message boards).<sup>2</sup> In the Prius owner’s manual, Toyota warns that people with implanted pacemakers or cardiac defibrillators should keep away from the vehicle smart entry and start system antennas.<sup>3</sup> Currently, the manual does not comment specifically about DBS. We recommend that such patients should not drive a Prius or other hybrid vehicle until more research and data are available for theirs and others safety. Whether they are safe as passengers remains to be proven. Further investigation should include measurement of all electromagnetic fields and frequencies generated in hybrid and electric cars, including the Toyota Prius, and evaluating for deep brain stimulator device interference or malfunction.

Charlene Chen, MD  
 Wendy Cole, RN MSN  
 Department of Neurology and Neurological Sciences  
 Stanford University  
 Stanford, California, USA

Potential conflicts of interest: The authors report no conflict of interest.

Published online 18 September 2009 in Wiley InterScience (www.interscience.wiley.com). DOI: 10.1002/mds.22739

Review article

# Hereditary progressive dystonia with marked diurnal fluctuation

Masaya Segawa \*

*Segawa Neurological Clinic for Children, 2–8 Surugadai Kanda, Chiyoda-ku, Tokyo 101-0062, Japan*

## Abstract

Hereditary progressive dystonia with marked diurnal fluctuation (HPD) is a dopa-responsive dystonia, now called autosomal dominant GTP cyclohydrolase 1 deficiency or Segawa disease, caused by mutation of the GCH-1 gene located on 14q22.1 to q22.2. Because of heterozygous mutation, partial deficiency of tetrahydrobiopterin affects tyrosine hydroxylase (TH) rather selectively and causes decrease of TH in the terminals of the nigrostriatal dopamine (NS DA) neurons, projecting to the D1 receptors on the striosome, the striatal direct pathways and the subthalamic nucleus (STN) and the D4 receptors of the tuberoinfundibular tract. The activities of TH in the terminal are high in early childhood decrease exponentially to the stationary level around early twenties, and show circadian oscillation. TH in HPD follows these variations with around 20% of normal levels and with development of the downstream structures show appears characteristic clinical symptoms age dependently.

In late fetus period to early infancy, through the striosome-substantia nigra pars compacta pathway failure in morphogenesis of the DA neurons in substantia nigra, in childhood around 6 years postural dystonia through the D1 direct pathways and the descending output of the basal ganglia. Diurnal fluctuation is apparent in childhood but decrease its grade with age.

TH deficiency at the terminal on the STN causes action dystonia from around 8 years and postural tremor from around 10 years, focal dystonia in adulthood.

Adult onset cases in the family with action dystonia start with writer's cramp, torticollis or generalized rigid hypertonus with tremor but do not show postural dystonia. TH deficiency on the D4 receptors causes stagnation of the body length in childhood. With or without action dystonia depends on the locus of mutation. Postural dystonia is inhibitory disorder, while action dystonia is excitatory disorder. The TH deficiency at the terminal does not cause morphological changes or degenerative process. Thus, levodopa shows favorable effects without any relation to the duration of illness.

© 2010 Published by Elsevier B.V. on behalf of the Japanese Society of Child Neurology.

*Keywords:* Autosomal dominant GCH-1 deficiency; Segawa disease; Postural type; Action type; Pteridine metabolism

## 1. Introduction

Hereditary progressive dystonia with marked diurnal fluctuation (HPD) is a dopa-responsive dystonia described by Segawa et al. in 1976 [1]. After discovery of the causative gene, the gene of GTP cyclohydrolase 1 (GCH-1) located on 14q22.1 to q22.2 [2], this is called as autosomal dominant GCH-1 deficiency or

Segawa disease. Clinically there are two types, postural dystonia and action dystonia type [3,4]. It depends on the family or the loci of mutation. In postural type the clinical symptoms are similar inter- and intra-families, however, action type shows intra-familial variations.

In this article clinical characteristics, neurophysiological, biochemical, neuroimaging, and neuropathological findings are reviewed. Pathophysiologies of these two types are discussed. Lastly, the pathophysiology of the early onset cases, another phenotype are commented.

\* Tel.: +81 3 3294 0371; fax: +81 3 3294 0290.  
E-mail address: segawa@segawa-clinic.jp



## 2. Clinical characteristics

In most cases the symptoms at onset is dystonic posture, with rigidity in one lower extremity, pes equinovarus, around 6 years. Clinical course was clarified by an experience of 51 years female with postural type having clinical course of 43 years after onset at 8 years, that is postural dystonia expands to other limbs, and all limbs and trunk muscles are affected by late teens, the rigidity aggravates progressively until around 20 years of age, but the progression subsides in twenties and becomes stationary in the thirties. Postural tremor with high cycles of 8–10 Hz appears after 10 years in an upper extremity and expands to all limbs by thirties. However, locomotion is preserved throughout the course.

In action dystonia type besides postural dystonia dystonic movements of an upper extremity or action retrocollis appear around 8 years. The latter may associate oculogyric crises. From experiences of 38 years female patients with 30 years clinical course and of a childhood onset case with long term follow up, torticollis and writer's cramp appear in adulthood. In families with action dystonia type, there are adult onset cases who start with writer's cramp, torticollis or generalized rigid hypertonus with postural tremor, but do not show dystonic posture or apparent progression.

Symptoms show marked diurnal fluctuation in childhood. But it attenuates the grade with age and becomes unapparent with cessation of clinical progression. In adult onset cases it is not observed. Childhood onset cases show stagnation of body length with onset of dystonia. This is not observed in cases with onset after adolescence.

A few patients show migraineous headache, autistic features, depressive reaction or obsessive behavior. Patients with onset early in infancy start with delay in motor and psychomotor development.

Childhood onset cases show marked female predominance. In our personal cases (41 cases from 20 families) F:M is 33:8, that is 4:1, and it is more marked in postural type 18:1 than action type 2:1. While adult onset cases show male predominance. Furukawa et al. [5] showed higher penetrance (87%) in females than males (38%).

Neurological examinations reveal rigid hypertonus [3,4]. But in contrast to Parkinson disease (PD) it is not plastic rigidity, and cases with tremor do not show cogwheel rigidity. These clinical signs, particularly rigidity and tremor, show asymmetry. Exaggeration of tendon reflexes, some with ankle clonus, are observed in child patients, however Babinski sign is negative. In advanced stage, pulsion is observed but freezing phenomenon is not detected because of preservation of locomotion. Cerebral or cerebellar signs or sensory abnormalities are not observed. Early onset patients show postural or truncal hypotonia, failure in locomotion

in infancy, camptocormia in late childhood and parkinsonism in adulthood besides symptoms of HPD.

In child onset cases, a dose of 20 mg/kg/day of plain levodopa (levodopa without decarboxylase inhibitor) or 4–5 mg/kg/day with decarboxylase inhibitor show complete and sustained effects without side effects [3,4,6]. There are families in which plain levodopa is effective throughout the course. However, in other family, replacement to L-dopa with decarboxylase inhibitor is necessary from around 13 years, because of activation of the decarboxylation of dopa in the intestine [6]. In a few cases choreic movements develop by a rapid increase of dosage or by administration of a high dose of levodopa in initial stage of treatment [4]. In these patients by reduction of the dosage and slow titration to the optimal doses, favorable and sustained effect is obtained without unfavorable side-effects [6].

However, for action dystonia and related symptoms effects of levodopa may be incomplete, and action retrocollis and oculogyric crises may be aggravated by initial doses [3,4]. Furthermore, patients with this type may show levodopa induced dyskinesia.

The short stature caused by stagnation of the body length recovers completely, if levodopa is administered before adolescent.

Anticholinergics showed a marked and sustained effect for dystonia, but not for tremor [3]. Moderate effects of tetrahydrobiopterin (BH<sub>4</sub>) with levodopa were reported, but no favorable effects with monotherapy [3].

Before the era of L-dopa stereotactic operations were performed on two patients, one patient with postural type dystonia [7] and the other with action type reported as juvenile parkinsonism [8] whose GCH-1 mutations were identified later [7,8]. Pallidotomy showed moderate effects on postural dystonia but not on tremor [7]. Ventrolateral thalamotomy was effective on tremor [7], rigidity and levodopa induced dyskinesia occurring in adult with action type [8], but no effect on postural dystonia [7].

The age related clinical course observed in a case with long clinical course is explained by following the age variation of the activities of tyrosine hydroxylase (TH) in the synaptic terminals of the caudate nucleus of the nigrostriatal (NS) DA neurons shown by McGeer and McGeer [9] with low levels of TH (Fig. 1). TH activities of the NS DA neurons do not show the state dependent variation in the SNc while show circadian oscillation in the terminals [9]. These evidences implicated that HPD is caused by non-progressive decrease of TH activities in the terminals of the NS DA neuron and develops clinical symptoms following the age and circadian variation of the TH activities of the terminals.

## 3. Studies for evaluation of the pathophysiology

Polysomnographies (PSGs) performed to clarify the sleep effects [3,4] revealed importance of REM sleep

### Age Variation of the Tyrosine Hydroxylase Activities of the Terminal of the Caudate nucleus vs the Clinical Course of HPD

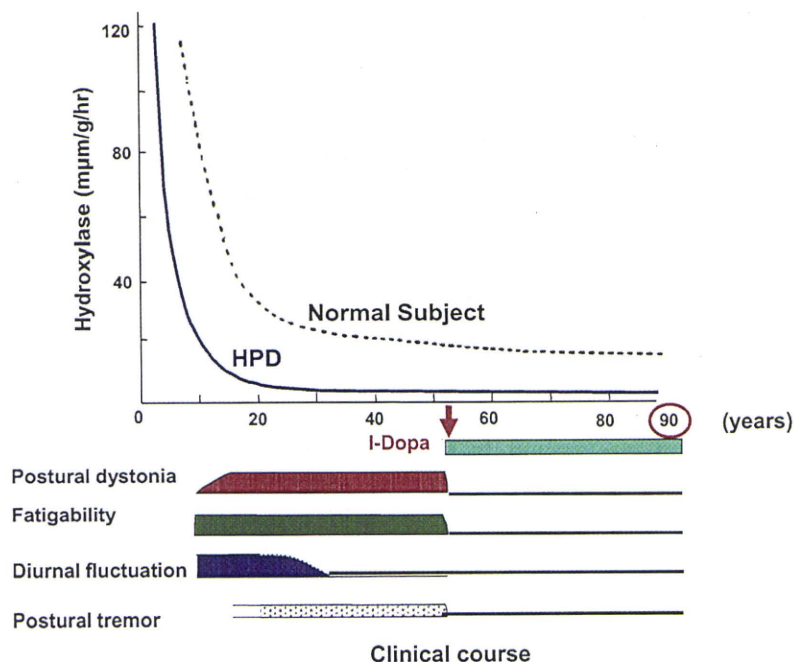


Fig. 1. Correlation of the 43 years clinical course of 51 years female postural type, with onset at 8 years and the age variation of the tyrosine hydroxylase activities of the terminals of the nigrostriatal dopamine neuron as the causative nucleus shown by McGeer and McGeer [9]. This case was completely recovered by L-dopa started at 51 years which continued without any side effects until 90 years.

(sREM) for the sleep effects by selective sleep stage deprivation studies [1]. Twitch movements (TMs) in sREM reflect the dopamine (DA) activities. In normal subjects TMs in sREM increase with sleep cycle and decrease with age. Degree of increment with sleep cycle reduces with age. The TMs of HPD patients followed these nocturnal and age variation with the lower levels of around 20% of normal values. In sREM of the 1st cycle it was markedly decreased less than 20% of the level in the last cycle of normal subjects, but in that of last cycle it exceeded more than 20%, which related morning recovery. Other parameters modulated by the brainstem aminergic neurons were preserved normally [3,4].

Fujita and Shintaku [10] revealed marked decrease less than 20% of the normal range of bipterin and neopterin in cerebrospinal fluid (CSF) of a case with HPD, by Furukawa et al. [11] confirmed the results and deficiency of GCH-1 was clarified as the cause of HPD [11]. In asymptomatic carriers these were 30–50% of normal levels. The activities of GCH-1 in the mononuclear blood cells decreased to less than 20% of normal levels in patients and 30–40% in asymptomatic carriers [2].

Ichinose found the gene of GCH-1 on 14q22.1 to q22.2 and examining seven HPD patients revealed this gene as the causative gene of HPD [2].

Neuroimaging, neurophysiological, neuropathological and neurohistological studies confirmed the pathophysiology speculated from clinical studies.

Magnetic resonance imaging (MRI) studies performed in various institutions revealed no abnormalities [3,4]. Brain positron emission tomography (PET) scans studies showed no definite abnormalities in [ $^{18}\text{F}$ ] dopa uptake, [ $^{11}\text{C}$ ] raclopride PET, [ $^{11}\text{C}$ ] N-spiperone PET [3] and normal development of the  $\text{D}_2$  receptors in HPD [3,4]. In our experience of two 38 years, female patients of action type with 30 years' clinical courses without treatments after the onset at 8 years, and one 59 years male with onset at 58 years showed normal [ $^{18}\text{F}$ ] dopa uptake and [ $^{11}\text{C}$ ] N-spiperone PET. These confirmed decrease of TH as the cause of DA deficiency.

Evaluations of voluntary saccades revealed abnormalities in both visually guided (VGS) and memory guided saccades (MGS), and implicated involvement of both the direct and the indirect pathways of the basal ganglia [12]. In adult onset patients abnormalities were observed only in MGS.

Paired pulse transcranial magnetic stimulation was studied in two institutes [13,14]. One study showed residual abnormalities in motor inhibition in levodopa-treated HPD patients even though clinically asymptomatic [13]. However, the other study revealed that dysfunction of GABA<sub>A</sub> inhibitory interneurons of the primary motor cortex does not contribute to the generation of postural dystonia of HPD [14]. Sensory evoked potential revealed normal gating in patients with postural type, while it was abnormal in patients with action type.

These neurophysiological studies revealed involvement of the striatal direct pathway and the descending output of the basal ganglia for the postural type and the indirect pathway and the ascending pathway for tremor and symptoms of action type dystonia.

Neuropathological and neurohistochemical studies were performed on a case with action dystonia reported as juvenile parkinsonism [8] and a 19 years old DRD female, postural type died by traffic accident [15], both of which were later confirmed GCH-1 gene mutation.

Neuropathological examinations revealed decrease in melanin, particularly in the ventral tier of the pars compacta of the substantia nigra (SNc) [8,15], and one with morphological immaturity of the neurons [8]. Histochemically, DA content was subnormal [16] or normal [8] in the SNc, while it showed marked decrement in the striatum [8,16]. The reduction was greater in the putamen than in the caudate nucleus, and subregionally, the decrement was more great in the rostral caudate and the caudal putamen similar to PD. However, in contrast to PD this case showed a greater DA loss in the ventral subdivision of the rostral caudate, the area rich in striosome, than its dorsal counterpart, though in the putamen, the dorsoventral DA gradient was similar to PD [16]. The activity and protein content of TH was decreased in the striatum, but within normal range in the SNc [16].

Furukawa et al. [17] showed marked reduction of total bipterin (84%) and neopterin (62%) in the putamen, despite normal concentration of aromatic acid decarboxylase, DA transporter and vesicular monoamine transporter. These authors [18] also demonstrated modest reduction of TH protein (52%) and DA (44%), despite marked reduction of striatal bipterin (82%) in an asymptomatic carrier, and implicated the levels of TH protein as a key for development of symptoms.

Up to now more than one hundred independent mutations have been identified in the coding region of GCH-1 which is identical in one family, but differs among families [2–4]. However, we found two occasions showing identical mutation in unrelated families.

It was shown molecular analysis remains unable to determine mutations in the coding region of the gene in approximately 40% of subjects with GCH-1 deficiency. In these cases, abnormalities in intron genomic deletion, a large gene deletion, an intragenic duplication or inversion of GCH-1 or mutation in as yet undefined regulatory gene modifying enzyme function may be present [3,4].

#### 4. Pathophysiological consideration

As for the pathogenetic mechanisms for dominant inheritance with heterozygous mutation, classic dominant negative effects have been considered [3,4]. The

rates of mutant GCH-1 messenger ribonucleic acid (mRNA) production against normal mRNA were 28% in a patient but 8.3% in an asymptomatic carrier [3,4]. However, the ratio varies depending on the locus of the mutation. Furthermore, the ratio differed among affected individuals in some families. These may cause inter- and intra-familial variation of the phenotype as well as the rate of penetrance. Furthermore, the loci of the mutation may also be involved in phenotype.

It is also necessary why a certain mutation relate particular clinical symptoms shown above.

As the enzyme for the synthesis of BH<sub>4</sub>, GCH-1 deficiency may affect tryptophan hydroxylase (TPH) as well as TH. There is the difference of  $K_m$  value for TH and TPH. With heterozygous mutant gene, the BH<sub>4</sub> decreases partially in HPD. Thus TH with higher affinity to BH<sub>4</sub> is affected rather selectively [3,4]. However, in molecular conditions with marked decrease of BH<sub>4</sub>, TPH is affected as well as TH and may produce symptoms induced by deficiencies of the 5HT neurons.

In basal ganglia disorders, contralateral or ipsilateral of the side of predominantly involved of the sternocleidomastoides (SCM) and the extremities reflects the region of the causative lesion.

In postural type of AD GCH-1 deficiency, predominant side of rigid hypertonus is contralateral between the SCM and the extremities. This suggests the lesion in the afferent structure to the striatum with side predominance ipsilateral to the predominantly affected side of the SCM, that is, involvement of the NS DA neuron with predominance to the side predominantly affected SCM.

Postural tremor, torticollis and generalized rigid hypertonus develop later independently from postural dystonia. The side predominance of these symptoms is ipsilateral both in the extremities and in the SCM. This implicates a causative lesion located in the downstream of the striatum. As these symptoms are DA responsive, it is suggested that hypofunction of the DA neuron projecting to the D<sub>1</sub> receptor on the subthalamic nucleus (STN) is postulated to be involved [3,4].

Furthermore, results of the stereotactic surgeries and the paired pulse transcranial magnetic stimulation show involvement of the ascending output of the basal ganglia in tremor, focal and segmental dystonia and rigidity in adult onset cases. These processes are also involved in focal dystonia.

Whereas, dopa-responsive growth arrest seen in children with HPD postulates the involvement of D<sub>4</sub> receptor of the tuberoinfundibular tract. The D<sub>4</sub> receptor belongs to the D<sub>2</sub> receptor family, which matures early among D<sub>2</sub> families [3,4]. This implicates that the terminals of the NS-DA neuron in HPD connect to the receptors which develop early.

Pteridine metabolism develops in late fetal period with critical period in early infancy which extends to

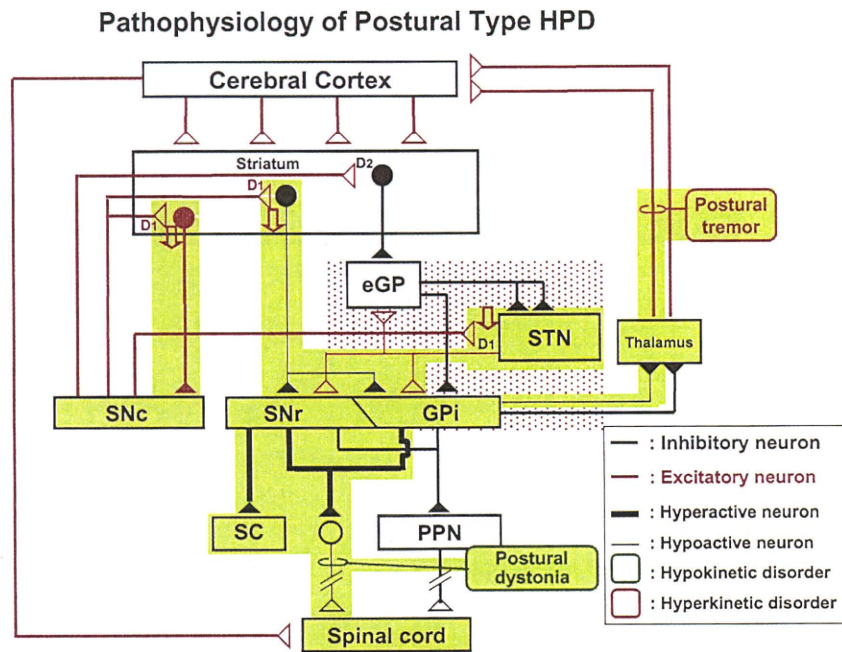


Fig. 2. Pathophysiologies of HPD; GPe: globus pallidus external segment; GPi: globus pallidus internal segment; STN: subthalamic nucleus; SNc: substantia nigra pars compacta; SN: substantia nigra pars reticulata; SC: superior colliculus; PPN: pedunculopontine nucleus.

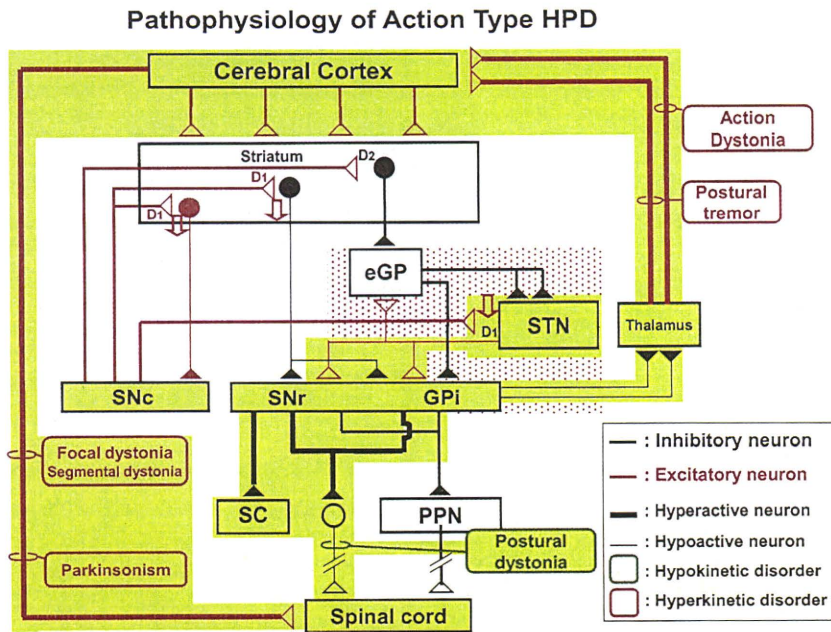


Fig. 3. Pathophysiologies of HPD; GPe: globus pallidus external segment; GPi: globus pallidus internal segment; STN: subthalamic nucleus; SNc: substantia nigra pars compacta; SN: substantia nigra pars reticulata; SC: superior colliculus; PPN: pedunculopontine nucleus.

early childhood [19]. Study in stimulated mononuclear blood cells [20] also showed age-dependent decrement of the activities of GCH-1 in the first three decades of life. Thus pteridine metabolism may involve in the age related decrement of TH activity [10] particularly in its early phase.

Thus, the pathophysiologies of postural and action type dystonia of HPD are shown in Figs. 2 and 3.

GCH-1 deficiency caused by abnormalities of pteridine metabolism leads to the decrease of the TH protein or DA in the ventral area of the striatum or the striosome in early developmental course.